Supplementary Information

Multifunctional CeO_2 incorporated Fe_2O_3 anchored on a rich porous structured carbon backbone for supercapacitors and Adsorption of Acid orange II

Hang Zhang,[a] Lijuan Xia,[a] Jianping Tang,[a] Yuan Li,[a] Lei Wang,[a*] Chuying Ouyang,[b*] Shengliang Zhong[a*]

[a] *Key Lab of Fluorine and Silicon for Energy Materials and Chemistry of Ministry of Education, College of Chemistry and Chemical Engineering, Jiangxi Normal University, Nanchang, 330022, China. E-mail: slzhong@jxnu.edu.cn*

[b] *Department of Physics, Laboratory of Computational Materials Physics, Jiangxi Normal University, Nanchang, 330022, P.R. China*

*corresponding author.

*E-mail: slzhong@jxnu.edu.cn

Table S1 Yield and productivity of the materials in the experiment.

Samples	m (g)			(g)	Rate
	m1 (g)	m2 (g)	m3 (g)		
Raw	0.09822	0.10038	0.09987	0.09949	/
Ce-DDA	0.08643	0.10032	0.09689	0.09455	95.03%
CF	0.06465	0.06889	0.07122	0.06825	68.60%
CFC	0.08066	0.08842	0.08454	0.08454	84.97%

Table S2 Samples and corresponding experiment parameters.

Sample	Reaction Temperature (°C)	Reaction Time (h)	n (Ce^{3+}) (mmol)	n($C_{12}H_{10}FeO_4$) (mmol)	Molar ratio of $C_{12}H_{10}FeO_4$ and Ce^{3+}
1	140	12	0.1	0.2	1:2
2	140	8	0.1	0.2	1:2
3	140	16	0.1	0.2	1:2
4	140	20	0.1	0.2	1:2
5	120	12	0.1	0.2	1:2
6	160	12	0.1	0.2	1:2
7	180	12	0.1	0.2	1:2
8	200	12	0.1	0.2	1:2
9	140	12	0.1	0.1	1:1
10	140	12	0.1	0.3	1:3
11	140	12	0.1	0.4	1:4
12	140	12	0.1	0.5	1:5

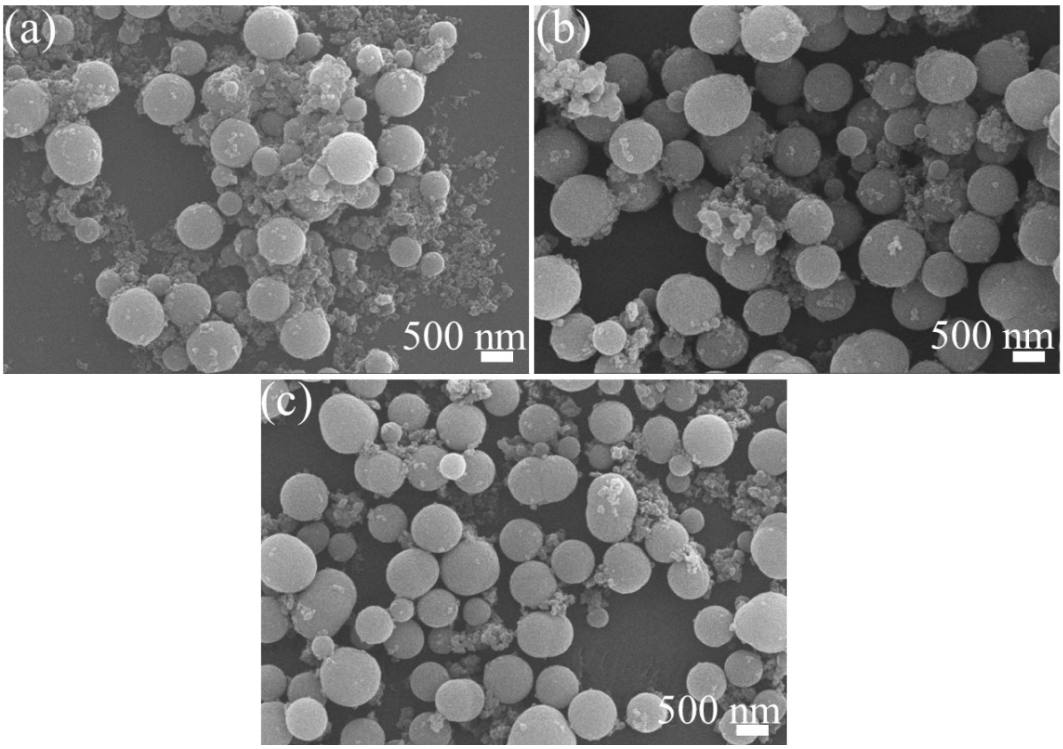

Fig. S1 SEM images of the precursor prepared at 140 °C for different times: (a) 8 h; (b) 16 h; (c) 20 h.

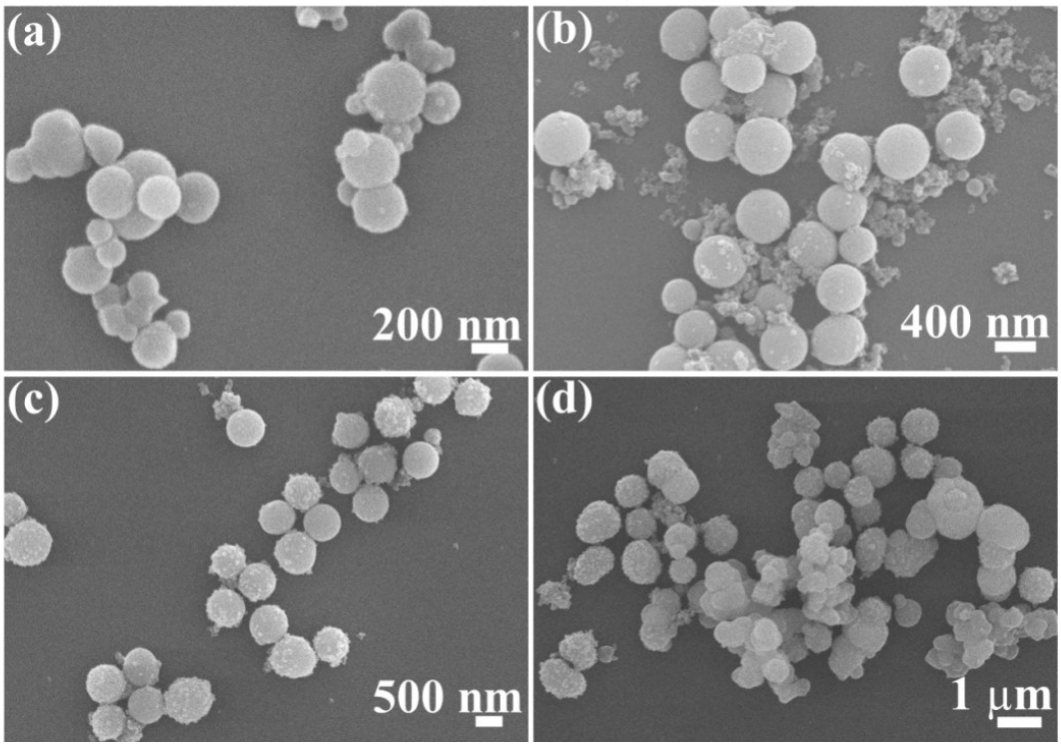

Fig. S2 SEM images of the precursor prepared at different temperature for 12 h : (a) 120 °C; (b) 160 °C; (c) 180 °C; (d) 200 °C.

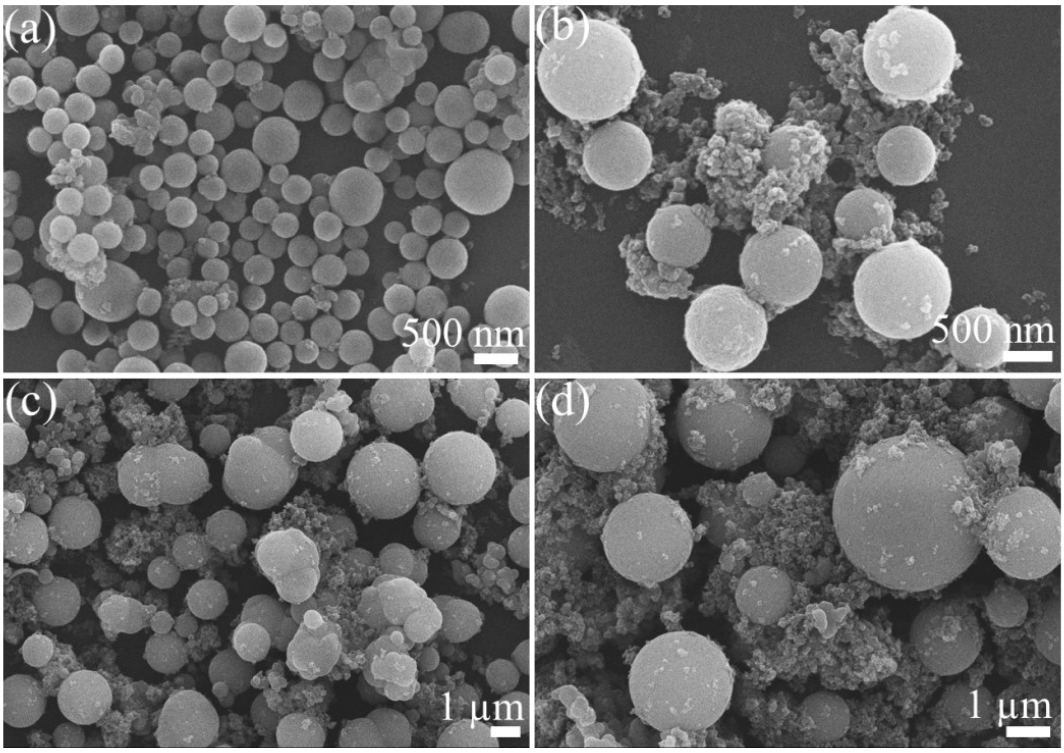

Fig. S**3** SEM images of the products prepared at 140 ^{o}C for 12 h with various molar ratios of $Ce(NO_3)_3 \cdot 6H_2O$ to $C_{12}H_{10}FeO_4$: (a) 1:1; (b) 1:3; (c) 1:4; and (d) 1:5.

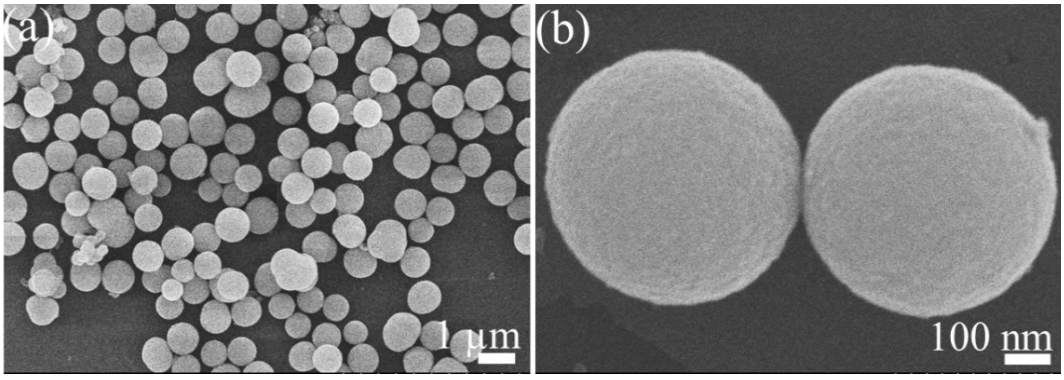

Fig. S4 (a, b) SEM images of the Ce-DDA precursor prepared at 140 ^{o}C for 12 h with $Ce(NO_3)_3 \cdot 6H_2O$ to $C_{12}H_{10}FeO_4$ = 1: 2.

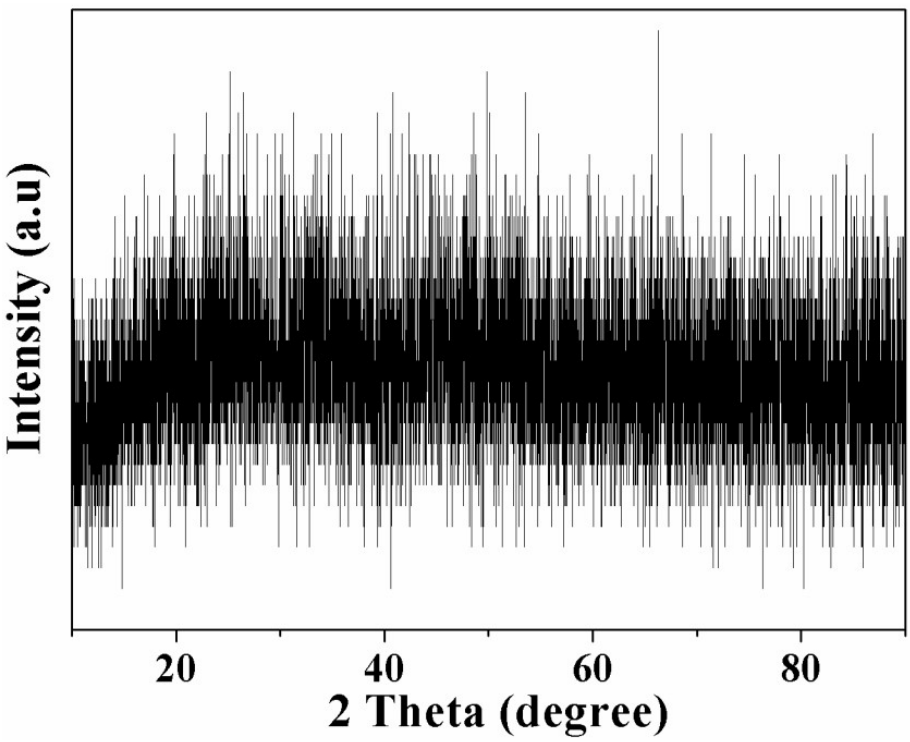

Fig. S5. XRD patterns of the precursor.

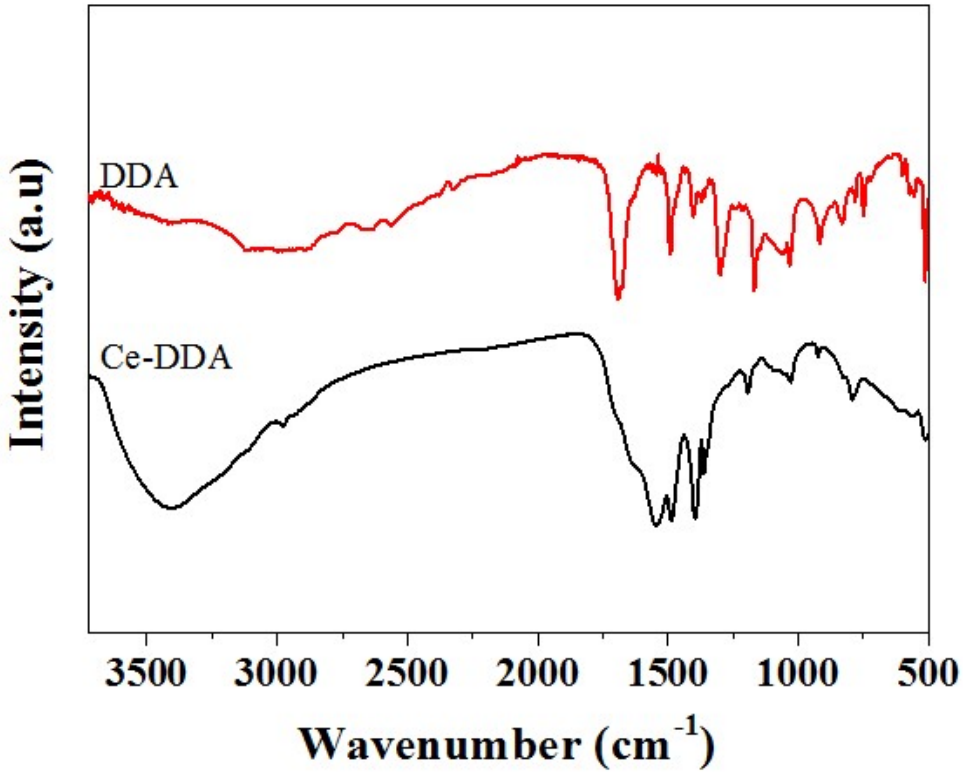

Fig. S6. FTIR patterns of the DDA ligand and Ce-DDA.

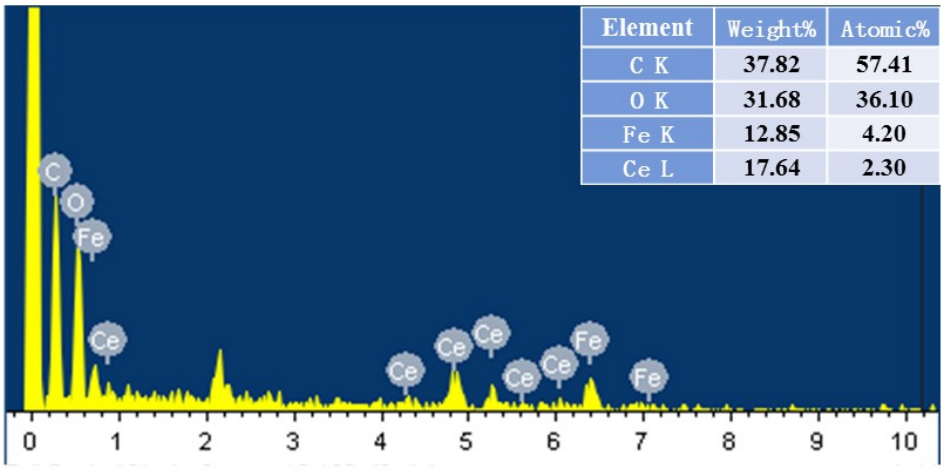

Fig. S7 EDS spectra of the Ce-DDA precursor.

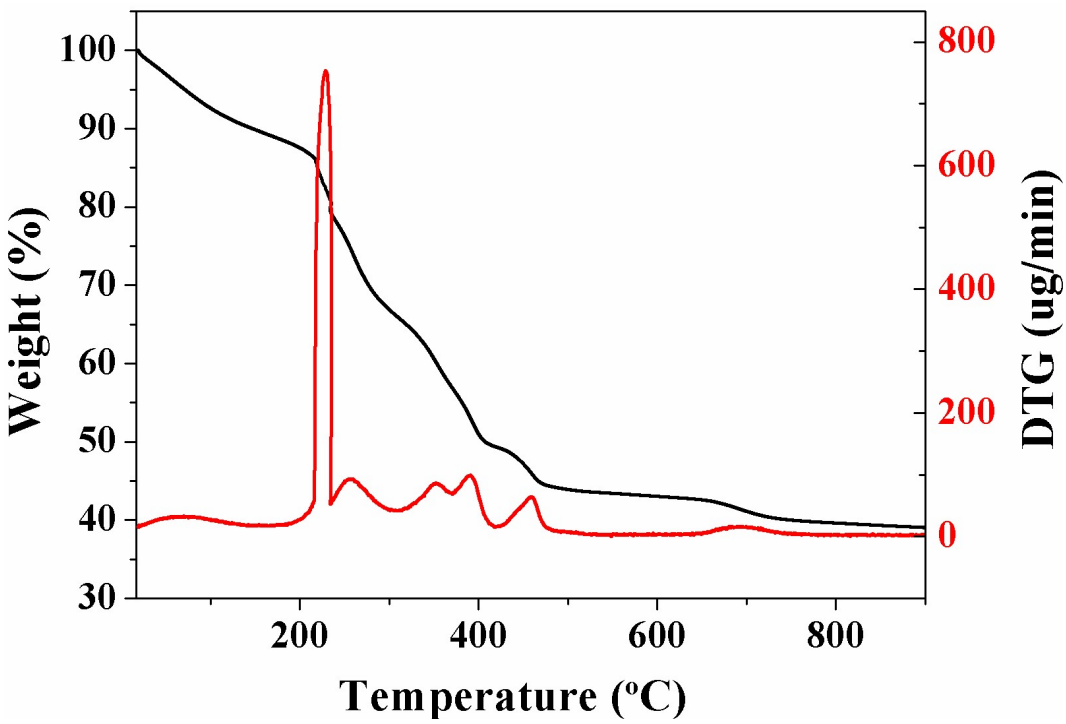

Fig. S8. TG-DTG curves of the precursor.

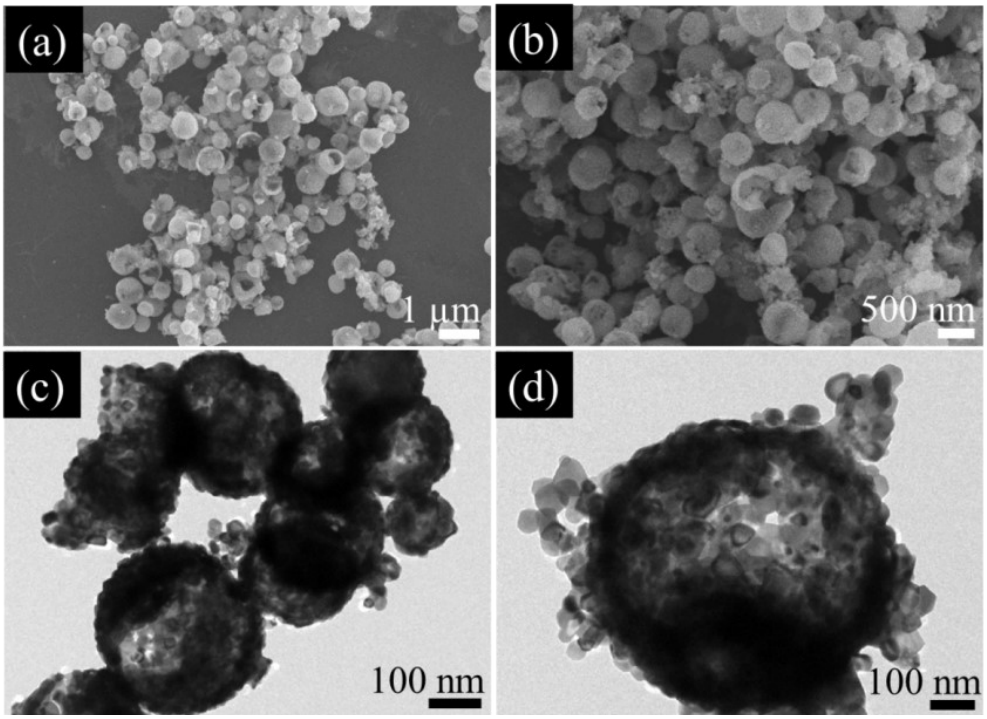

Fig. S9 SEM images and TEM images of CF obtained after calcination of the precursor in air at 800 °C for 4 h.

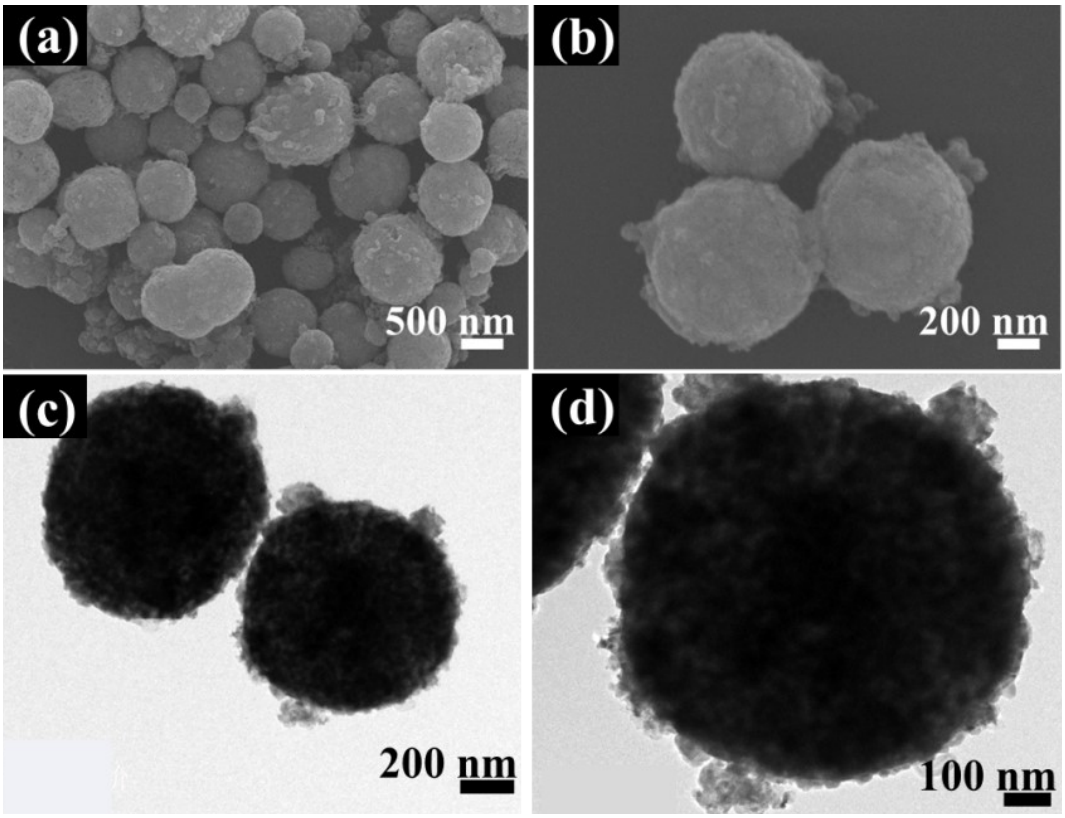

Fig. S10 SEM images and TEM images of CFC obtained after calcination of the precursor in N_2 at 800 °C for 4 h.

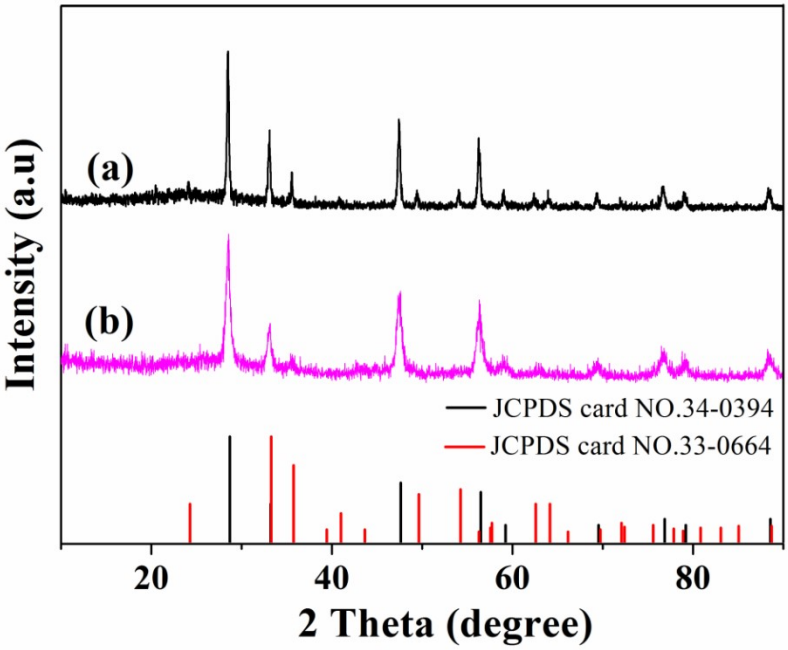

Fig. S11 The XRD patterns of the CF (a) and CFC (b) (CeO_2: JCPDS card 34-0394; Fe_2O_3: JCPDS card 33-0664).

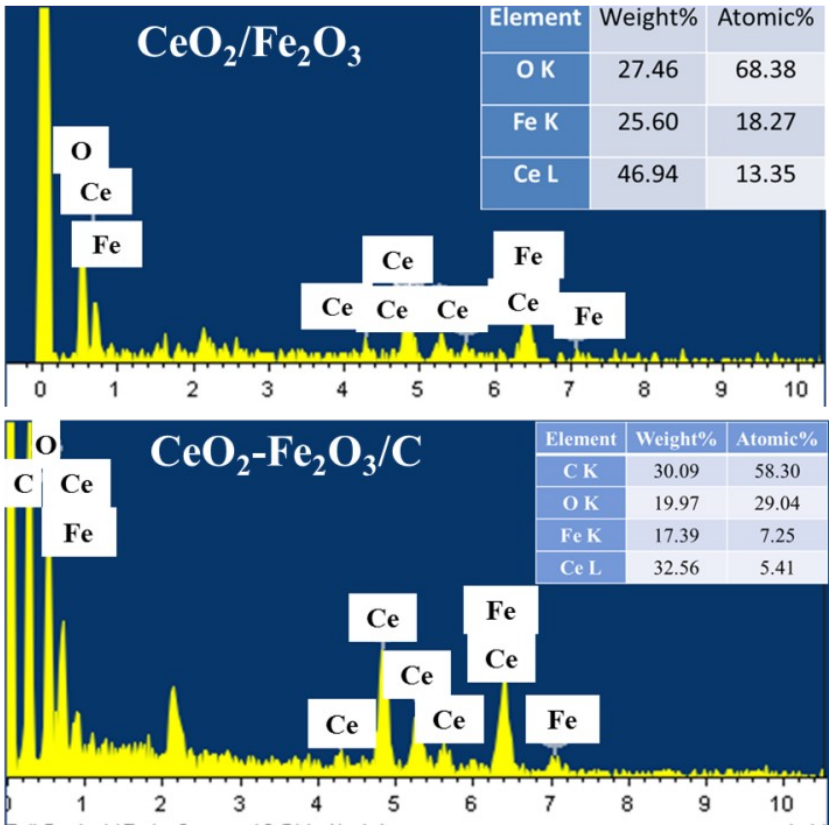

Fig. S12 EDX spectra of the as-prepared CF and CFC.

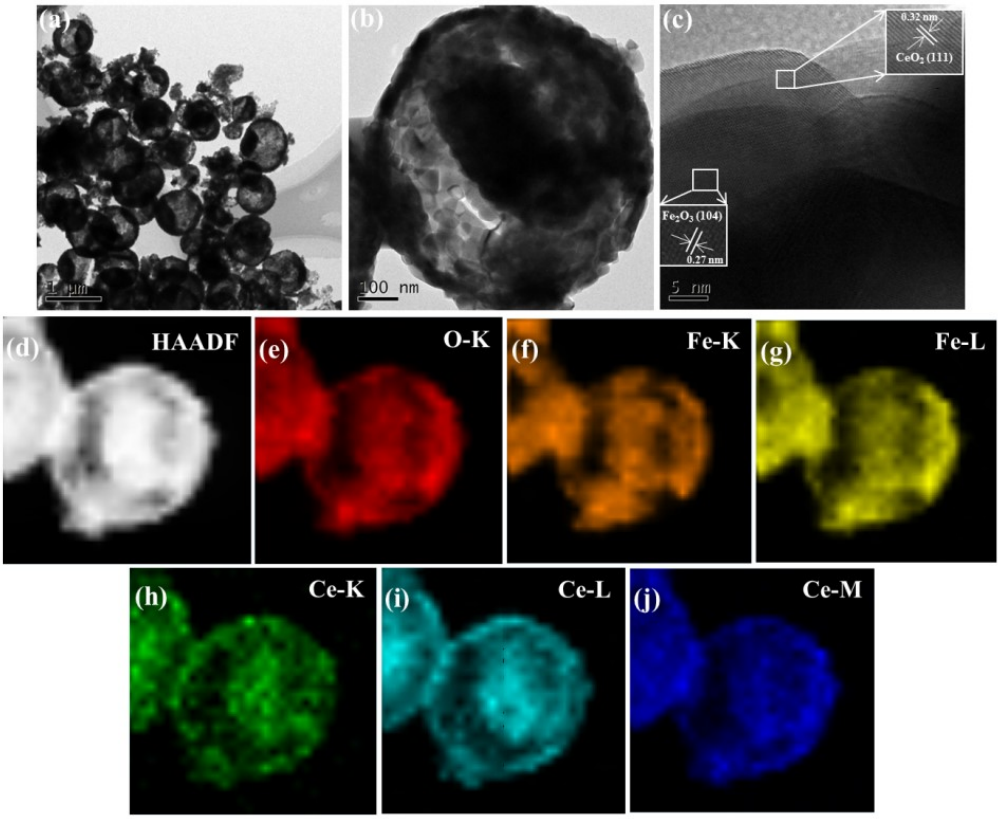

Fig. S13 TEM and element mapping of CF. a-b TEM image; (c) HRTEM of the selective area; (d) HAADF-S TEM image of CF; e-j: Element mapping of O, Fe and Ce.

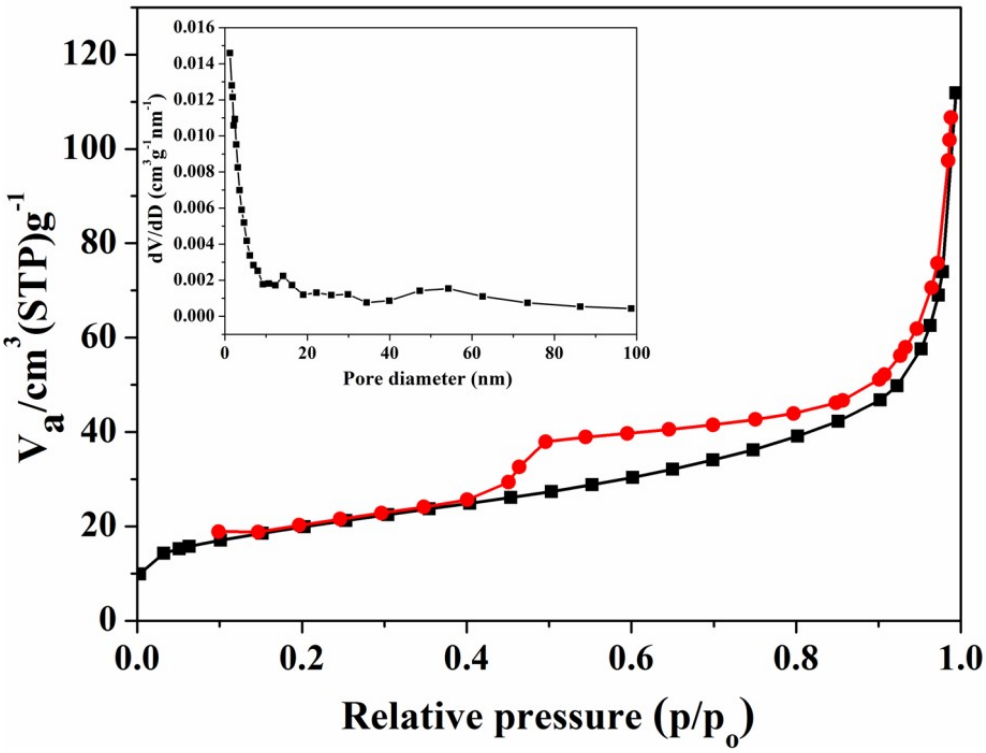

Fig. S14 Nitrogen adsorption-desorption isotherm of as-synthesized CFC; the inset is the corresponding BJH pore size distribution curve.

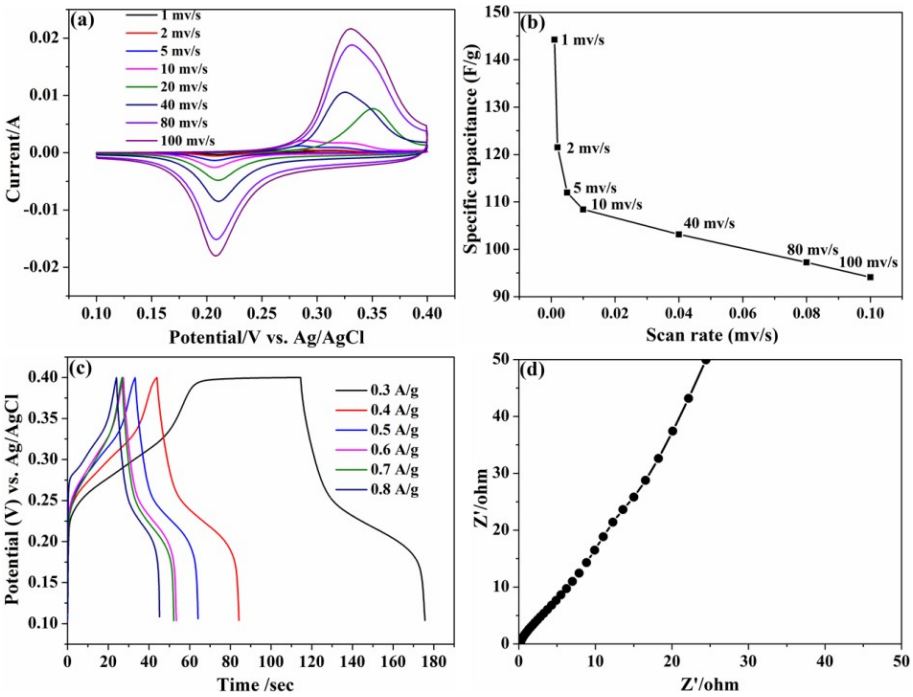

Fig. S15 a: Cyclic voltammetry curves; b: Comparison of specific capacitance at various scan rates of CF electrodes; c: Galvanostatic charge/discharge curves of CF at different current densities; d: Nyquist plots.

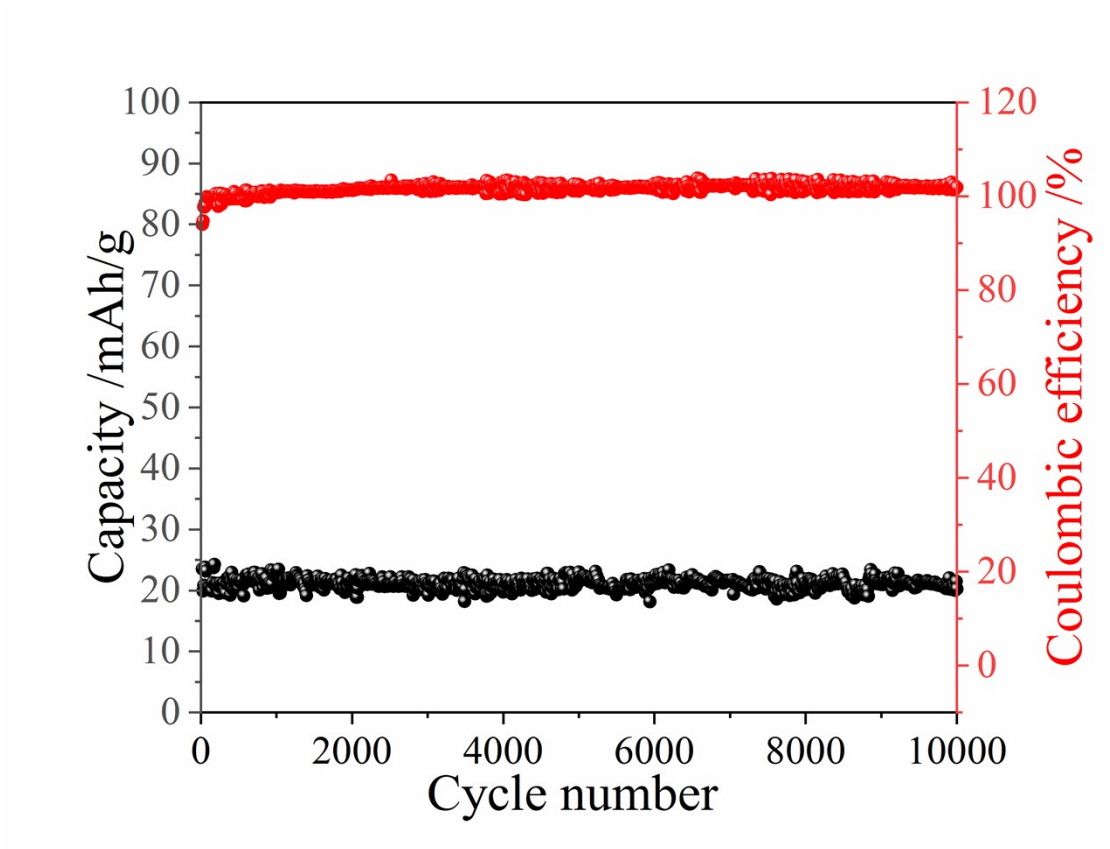

Fig. S16 Cycle performance of CFC electrode.

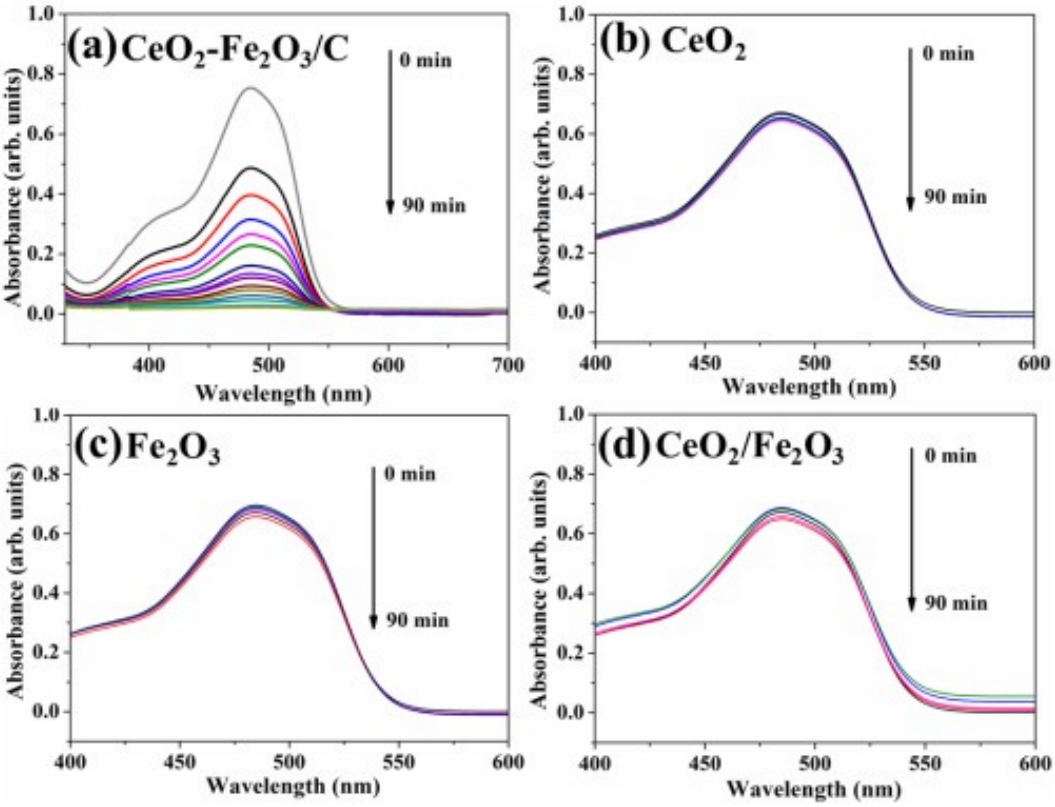

Fig. S17 The absorbance spectra (C_o=10 mg/L) on AO7 adsorption.